J|A|C|S ARTICLES

Published on Web 07/15/2009

Combined High-Resolution Neutron and X-ray Analysis of Inhibited Elastase Confirms the Active-Site Oxyanion Hole but Rules against a Low-Barrier Hydrogen Bond

Taro Tamada,[†] Takayoshi Kinoshita,[‡] Kazuo Kurihara,[†] Motoyasu Adachi,[†] Takashi Ohhara,[†] Keisuke Imai,[§] Ryota Kuroki,*[,†] and Toshiji Tada[‡]

Quantum Beam Science Directorate, Japan Atomic Energy Agency, 2-4 Shirakata-Shirane, Tokai, Ibaraki 319-1195, Japan, Department of Biological Science, Graduate School of Science, Osaka Prefecture University, 1-1 Gakuen-cho, Naka-ku, Sakai, Osaka 599-8531, Japan, and Lead Discovery Research Laboratories, Astellas Pharma, Inc., 21 Miyukigaoka, Tsukuba, Ibaraki, 305-8585, Japan

Received April 10, 2009; E-mail: kuroki.ryota@jaea.go.jp

Abstract: To help resolve long-standing questions regarding the catalytic activity of the serine proteases, the structure of porcine pancreatic elastase has been analyzed by high-resolution neutron and X-ray crystallography. To mimic the tetrahedral transition intermediate, a peptidic inhibitor was used. A single large crystal was used to collect room-temperature neutron data to 1.65 Å resolution and X-ray data to 1.20 Å resolution. Another crystal provided a low-temperature X-ray data set to 0.94 Å resolution. The neutron data are to higher resolution than previously reported for a serine protease and the X-ray data are comparable with other studies. The neutron and X-ray data show that the hydrogen bond between His57 and Asp102 (chymotrypsin numbering) is 2.60 Å in length and that the hydrogen-bonding hydrogen is 0.80−0.96 Å from the histidine nitrogen. This is not consistent with a low-barrier hydrogen which is predicted to have the hydrogen midway between the donor and acceptor atom. The observed interaction between His57 and Asp102 is essentially a short but conventional hydrogen bond, sometimes described as a short ionic hydrogen bond. The neutron analysis also shows that the oxygen of the oxopropyl group of the inhibitor is present as an oxygen anion rather than a hydroxyl group, supporting the role of the "oxyanion hole" in stabilizing the tetrahedral intermediate in catalysis.

Introduction

Elastase is a serine protease classified in the chymotrypsin family, and is possibly the most destructive enzyme having the ability to degrade virtually all of the connective components in the body. Uncontrolled proteolytic degradation by elastase has been implicated in a number of pathological conditions. Pancreatic elastase (EC 3.4.21.36) causes the fatal disease pancreatitis, and leukocyte elastase (EC 3.4.21.37) has been implicated in a number of inflammatory disorders. Structure based drug design (SBDD) using X-ray structure of porcine pancreatic elastase (PPE) with its selective inhibitors have been researched. Nevertheless, it is hard to develop the highly selective drugs for each elastase which can suppress the side effects due to other elastases.

The catalytic mechanism of chymotrypsin-like serine proteases has been the subject of much investigation.[1−3] Three amino acids, histidine, aspartic acid, and serine (His57, Asp102, and Ser195; residues are numbered based on homology to chymotrypsin), compose the "catalytic triad" or "charge relay system" conserved in the active site of serine proteases. The first step of catalysis begins with a nucleophilic attack upon the carbonyl group of substrate by the Oγ atom of Ser195.[2] Consequently, in the second step of catalysis, a tetrahedral intermediate is formed via covalent bonding of Ser195 to the substrate carbonyl group. This tetrahedral intermediate is electrostatically stabilized through hydrogen bonds with the backbone amides of Gly193 and Ser195, together forming an "oxyanion hole".[3] The nucleophilicity of Ser195 is hypothesized to increase via a "low barrier hydrogen bond (LBHB)" formed between the side chains of His57 and Asp102.[4−6] The tetrahedral intermediate collapses to acyl-enzyme intermediate by expulsion of leaving group assisted by proton of His57.

Although the primary and tertiary structures of chymotrypsin/trypsin-type proteases are quite different from the subtilisin type proteases, it is known that three-dimensional geometry of the His-Asp-Ser catalytic triad is conserved. The existence of a LBHB in the catalytic triad of these two serine proteases has been experimentally evaluated by subangstrom X-ray crystallography and NMR measurements. The 0.78 Å resolution structure (PDB ID: 1GCI) analysis of subtilisin supported the existence of a LBHB by locating the position of a hydrogen

[†] Japan Atomic Energy Agency.
[‡] Osaka Prefecture University.
[§] Astellas Pharma, Inc.

(1) Hedstrom, L. *Chem. Rev.* **2002**, *102*, 4501–4524.
(2) Hess, G. P.; McConn, J.; Ku, E.; McConkey, G. *Philos. Trans. R. Soc. London, Ser. B* **1970**, *257*, 89–104.
(3) Henderson, R. *J. Mol. Biol.* **1970**, *54*, 341–354.
(4) Cleland, W. W.; Kreevoy, M. M. *Science* **1994**, *264*, 1887–1890.
(5) Frey, P. A.; Whitt, S. A.; Tobin, J. B. *Science* **1994**, *264*, 1927–1930.
(6) Cleland, W. W.; Frey, P. A.; Gerlt, J. A. *J. Biol. Chem.* **1998**, *273*, 25529–25532.

10.1021/ja9028846 CCC: $40.75

Table 1. Hydrogen Bond Geometries between His-Asp in the Catalytic Triad in Serine Proteases

	Nδ1···Oδ2 (Å)	Nδ1−D(H)δ1 (Å)	D(H)δ1···Oδ2 (Å)	Nδ1−D(H)δ1···Oδ2 (deg)
PPE/FR130180[a] (1.65 Å neutron, pD 5.0)	2.60	0.96	1.65	172
PPE/FR130180[a] (0.94 Å X-ray, pH 5.0)	2.60	0.80	1.82	166
Trypsin/MIP[b] (1.80 Å Neutron, pH 6.2[c], 1NTP[d])	2.48	1.03	1.63	137
Trypsin (0.83 Å X-ray, pH 5.0, 1PQ5[d])	2.75	0.86	1.91	165
Subtilisin (0.78 Å X-ray, pH 5.9, 1GCI[d])	2.64	1.12	1.57	157
αLP (0.83 Å X-ray, pH 8.0, 1SSX[d])	2.77	0.83	1.95	170
αLP (0.82 Å X-ray, pH 5.0, 2H5C[d])	2.76	0.85	1.93	164
αLP/boroVal(gol)[e] (0.90 Å X-ray, pH 8.0, 2H5D[d])	2.73	1.01	1.77	159

[a] This study. [b] Monoisopropyl ester phosphonic acid. [c] Uncorrected pH meter reading values.[28,29] [d] These values are calculated using each coordinate of PDB code. [e] BoroVal(gol): MeOSuc-Ala-Ala-Pro-boroVal−OH.

atom equidistant between the Nδ1 atom of histidine and the Oδ2 atom of aspartic acid,[7] but the location of the hydrogen atom seen in the subangstrom X-ray structure of trypsin[8] (PDB ID: 1PQ5) did not support a LBHB (Table 1). The NMR studies of chymotrypsin and peptidic compound showed a downfield shift of the Hδ1 signal of His57 suggesting the presence of a LBHB.[5] However, subangstrom X-ray crystallography of α-lytic protease (αLP) (which is structurally homologous to chymotrypsin) revealed that a short ionic hydrogen bond (SIHB), and not a LBHB, stabilized the transition state during catalysis.[9,10] Furthermore, NMR studies of αLP and subtilisin BPN′ proposed that unusual chemical shifts corresponded to a ring flip mechanism of His57 during catalysis and not to formation of a LBHB.[11,12]

Thus, the LBHB hypothesis in serine protease catalysis is still a matter of debate, and it is therefore important to directly observe this hydrogen atom location by neutron diffraction. To accomplish this goal, we employed peptidic inhibitor FR130180 (4-({(*S*)-1-[((*S*)-2-{[(*RS*)-3,3,3-trifluoro-1-isopropyl-2-oxopropyl]-aminocarbonyl}pyrrolidin-1yl)carbonyl]-2-methylpropyl}amino-carbonyl) benzoic acid) a peptidyl fluonated ketone known to be an excellent inhibitor of the elastases.[13−15] Kinetic analysis of fluorinated ketones suggests that these compounds are transition-state analogue inhibitors. In the complex structure between PPE and FR130180, the carbonyl in FR130180 is converted to the tetrahedral structure mimicking the catalytic transition intermediate. Here, we report the structures of PPE in complex with peptidic inhibitor FR130180 determined by neutron diffraction at 1.65 Å resolution and by X-ray diffraction at 0.94 Å resolution. SIHB, not a LBHB, is located between the active site His57 and Asp102 catalytic residues. In addition, the structural information including hydrogen positions will provide additional knowledge to improve inhibitor design.

Methods

Crystallization. Crystallization of PPE/FR130180 complex was performed as described previously.[16] For neutron diffraction study, a crystal with dimensions of 2.9 × 1.4 × 1.2 mm (∼3.3 mm^3) was obtained by repeated macroseeding under deuterated solution over a period of four months.

Data Collection. Neutron data collection was performed at the 1G-A site of the JRR-3 reactor at Japan Atomic Energy Agency, Tokai, Japan. The crystal obtained as described above was sealed in a quartz capillary for neutron diffraction studies. Reflections were collected at room temperature using a monochromatic neutron beam (λ = 2.9 Å) and were recorded on a neutron imaging plate at the BIX-3 single crystal diffractometer.[17] Diffraction data from rotation about two independent axes was merged to obtain a complete data set. A total rotation range of 166.8°, comprising 556 oscillation images with exposure time of 4 h/frame, was collected using individual rotation angles of 0.3°. Intensity data were processed using the programs DENZO and SCALEPACK.[18] The full data set was integrated and scaled to 1.65 Å resolution. The total number of observed reflections was 73 039 and these were merged into 24 296 unique reflections with an R_{merge} of 0.098 (R_{merge} in the highest resolution shell of 0.328).

X-ray data collection at room temperature using the same crystal after neutron data collection was performed at beamline BL6A at the Photon Factory (PF), Tsukuba, Japan. Reflections were collected using a monochromatic X-ray beam (λ = 1.00 Å) and were recorded on a Quantum-4R detector of Area Detector Systems Corporation (ADSC) (Poway, CA) with a total rotation range of 180°. Intensity data were processed using the program HKL2000.[18] A full data set was integrated and scaled to 1.20 Å resolution. The total number of observed reflections was 425 212 and these were merged into 67 111 unique reflections with an R_{merge} of 0.050 (R_{merge} in the highest resolution shell of 0.391).

X-ray data collection at 100 K was performed at BL41XU at SPring-8, Hyogo, Japan. Reflections were recorded on an ADSC Quantum-315 detector with a total rotation range of 240° using a monochromatic X-ray beam (λ = 0.71 Å) from a crystal soaked in Paraton-N (Hampton Research, Aliso Viejo, CA) as a cryo-protectant and then flash-frozen in a nitogen-gas stream at 100 K. Intensity data were processed using HKL2000. A complete data set was integrated and scaled to 0.94 Å resolution. The number of total observed reflections was 1 171 606 and these were merged into 134 132 unique reflections with an R_{merge} of 0.072 (R_{merge} in the highest resolution shell of 0.392). Data collection and refinement statistics of neutron and X-ray diffraction studies are summarized in Table S1 of Supporting Information.

(7) Kuhn, P.; Knapp, M.; Solitis, S. M.; Ganshaw, G.; Thoene, M.; Bott, M. *Biochemistry* **1998**, *37*, 13446–13452.
(8) Schmidt, A.; Jelsch, C.; Østergaard, P.; Rypniewski, W.; Lamzin, V. S. *J. Biol. Chem.* **2003**, *278*, 43357–43362.
(9) Fuhrmann, C. N.; Kelch, B. A.; Ota, N.; Agard, D. A. *J. Mol. Biol.* **2004**, *338*, 999–1013.
(10) Fuhrmann, C. N.; Daughety, M. D.; Agard, D. A. *J. Am. Chem. Soc.* **2006**, *128*, 9086–9102.
(11) Ash, E. L.; Sudmeier, J. L.; De Fabo, E. C.; Bachovchin, W. W. *Science* **1997**, *278*, 1128–1132.
(12) Ash, E. L.; Sudmeier, J. L.; Day, R. M.; Vincent, M.; Torchilin, E. V.; Haddad, K. C.; Bradshaw, E. M.; Sanford, D. G.; Bachovchin, W. W. *Proc. Natl. Acad. Sci. U.S.A.* **2000**, *97*, 10371–10376.
(13) Gelb, M. H.; Svaren, J. P.; Abeles, R. H. *Biochemistry* **1985**, *24*, 1813–1817.
(14) Imperiali, B.; Abeles, R. H. *Biochemistry* **1986**, *25*, 3760–3767.
(15) Stein, R. L.; Strimpler, A. M.; Edwards, P. D.; Lewis, J. J.; Mauger, R. C.; Schwartz, J. A.; Stein, M. M. B.; Abeles, R. H. *Biochemistry* **1986**, *25*, 3760–3767.
(16) Kinoshita, T.; Tamada, T.; Imai, K.; Kurihara, K.; Ohhara, T.; Tada, T.; Kuroki, R. *Acta Crystallogr., Sect. F: Struct. Biol. Cryst. Commun.* **2007**, *63*, 315–317.
(17) Tanaka, I.; Kurihara, K.; Chatake, T.; Niimura, N. *J. Appl. Crystallogr.* **2002**, *35*, 34–40.
(18) Otwinoski, Z.; Minor, W. In *Methods in Enzymology: Macromolecular Crystallography, Part A*; Carter, C. W., Jr., Sweet, R. M., Eds.; Academic Press: New York, 1997, Vol. 276; pp 307−326.

Refinement. Crystallographic refinement of the neutron structure was performed by the program PHENIX[19] in a joint refinement[20] using 1.2 Å X-ray and 1.65 Å neutron diffraction data collected at room temperature from the same crystal. X-ray structure at 0.94 Å resolution was used as a starting model of refinement. The $F_o - F_c$ omit map nuclear density showed that the hydrogens which bonded to nitrogen and oxygen atoms in the side chains were replaced by deuterium. The deuterium positions were determined based on the $F_o - F_c$ omit nuclear density. The model building and adjustment of hydrogen and deuterium location were performed by the programs COOT[21] and QUANTA (Accelrys, Inc., San Diego, CA). The Hydrogen (H)/Deuterium (D) exchange ratios for main chain amide hydrogens were determined by occupancy refinement using the program PHENIX. In addition, the deuterium atoms in the side chain of histidine residues and FR130180 were refined using relaxed geometry restraints. The final model, including a total of 4226 atoms (H and D atoms, 2172; non-H and D atoms, 2054), was refined to a crystallographic *R*-factor of 19.6% (free *R*-factor = 21.5%) using 23 486 reflections from neutron diffraction to 1.65 Å resolution.

Refinement with conjugate-gradient least-squares minimization at 0.94 Å resolution X-ray data was carried out using the program SHELXL-97[22] with model building and adjustment using QUANTA and COOT. A starting model was obtained by molecular replacement with the program AMORE[23] using the PPE coordinates from complex structure with another inhibitor (PDB ID: 1MMJ).[24] The $F_o - F_c$ electron densities calculated by initial phases clearly showed the existence of the FR130180 inhibitor bound within the active site. Hydrogen atoms were included in the model by SHELXL-97 as riding hydrogens. Finally, hydrogen atoms were rigidly placed on heavy atoms using the AFIX command which defines the generation of idealized coordinates of hydrogens and geometrical constraints in the refinement, but only hydrogens which bonded to nitrogen atoms in side chain of His residues were loosed from restraints using AFIX. In addition, restraints (DFIX and DANG commands which define the ideal distance and angle between two non-hydrogen atoms, respectively) of carboxyl atoms in Asp residues and benzoic acid moiety of FR130180 were released. The final model included 240 residues, one inhibitor, 414 water molecules, one calcium ion, and one sulfate ion. All riding hydrogens except for water molecules were added to the model to give a final crystallographic *R*-factor of 10.7% (free *R*-factor = 12.8%) using 127 267 reflections between 10.0 and 0.94 Å resolution. The atomic coordinate and structure factors of the neutron and subangstrom X-ray structures have been deposited in the Protein Data Bank, www.rcsb.org (PDB ID code 3HGN and 3HGP, respectively).

Results

Overall Structure of PPE/FR130180 Complex Determined Using Both Neutron and X-ray Diffraction. The tertiary structure of PPE complex with the peptidic inhibitor FR130180 was determined to 1.65 Å resolution by neutron crystallography and 1.20 Å resolution by X-ray crystallography at room temperature (RT) in a joint refinement using PHENIX from the same crystal (Figure 1A). In addition, the 0.94 Å resolution X-ray structure at 100 K was also determined using another crystal in order to compare the results. Table S1 in Supporting Information lists the statistics of their data collection and refinement. The refined coordinates (non-hydrogens) of the 1.65 Å neutron and the 0.94 Å X-ray structure of PPE/FR130180 complex have an expected minimal error of 0.015 Å and 0.004 Å, respectively, according to the calculation using the program SFCHECK.[25] The overall structure of PPE determined by neutron diffraction is essentially identical to the X-ray structures here and previously determined.[24] The root-mean-square deviation (rmsd) of PPE between neutron and X-ray structures for all/backbone atom locations excluding hydrogen and deuterium was 0.55/0.22 Å. The peptidic inhibitor FR130180 is covalently bound to the side chain of Ser195 of PPE. In this covalent complex, the carbonyl structure adjacent to the trifluoromethyl group in FR130180 is converted to the tetrahedral structure mimicking the catalytic transition intermediate state. The rmsd of FR130180 between the neutron and X-ray structures for all atoms excluding hydrogen and deuterium atoms is 0.53 Å.

Hydrogen Atoms of Neutron Structure. The complex structure including a total of 1792 hydrogen and deuterium atoms and 190 hydration water molecules was determined by neutron crystallography. The crystallization for neutron diffraction was performed in D_2O, and 435 hydrogen atoms in the PPE/FR13080 complex were substituted by deuterium atoms. The 1357 hydrogen atoms which bonded to carbon atoms were still assigned as hydrogen. The 203 hydrogen atoms which bonded to nitrogen and oxygen atoms in side chains and FR130180 were replaced by deuterium. The hydrogen atoms in backbone amides were treated as "H/D exchange" hydrogen (indicated as the term "D(H)" in this paper).[26] The 232 hydrogen atoms in PPE and FR130180 fell under this category. The average value of the occupancy of D was 0.66. There are correlations between the solvent accessibility of each residue and the H/D exchange ratios. Especially, non- and low exchanged region (occupancy of D = 0−0.3) localized on β-barrel structures (Figure 1B).

Inhibitor Recognition of PPE. The interaction between PPE and FR130180 is schematically shown in Figure 2. The inhibitor binds to PPE using four subsites (S1∼S4) among the classified subsites[27] and the corresponding groups bound in these subsites are defined to be P1∼P4, respectively.[24,27] The S1 subsite, most specific for recognition of substrate peptide,[27] is structurally complementary to, and forms extensive van der Waals interactions with, the isopropyl moiety of the FR130180 in the P1 position. The observation of hydrogen atoms revealed that the hydrophobic interactions of the isopropyl group of the FR130180 with the side chains of Thr213 and Val216 shows a characteristic "leucine zipper" like structure (Figure 3A). The distance between the C30 atom in the isopropyl group of the inhibitor P1 position and the Cγ2 atom of Thr213 in the enzyme is 3.53 and 3.58 Å in the subangstrom X-ray and neutron structure, respectively. The C29 atom in the same isopropyl group is 3.83/3.68 Å

(19) Adams, P. D.; Grosse-Kunstleve, R. W.; Hung, L. W.; Ioerger, T. R.; McCoy, A. J.; Moriarty, N. W.; Read, R. J.; Sacchettini, J. C.; Sauter, N. K.; Terwilliger, T. C. *Acta Crystallogr., Sect. D: Biol. Crystallogr.* **2002**, *58*, 1948–1954.
(20) Wlodawer, A.; Hendrickson, W. A. *Acta Crystallogr., Sect. A: Found. Crystallogr.* **1982**, *38*, 239–247.
(21) Emsley, P.; Cowtan, K. *Acta Crystallogr., Sect.D: Biol. Crystallogr.* **2004**, *60*, 2126–2132.
(22) Sheldrick, G. M.; Schneider, T. R. In *Methods in Enzymology: Macromolecular Crystallography, Part B*; Carter, C. W., Jr., Sweet, R. M., Eds.; Academic Press: San Diego, CA, 1997; Vol. 277, pp 319−343.
(23) Navaza, J. *Acta Crystallogr., Sect. A: Found. Crystallogr.* **1994**, *50*, 157–163.
(24) Kinoshita, T.; Nakanishi, I.; Sato, A.; Tada, T. *Biol. Med. Chem. Lett.* **2003**, *13*, 21–24.
(25) Vaguine, A. A.; Richelle, J.; Wodak, S. J. *Acta Crystallogr., Sect. D: Biol. Crystallogr.* **1999**, *55*, 191–2051.
(26) Bennett, B.; Langan, P.; Coates, L.; Mustyakimov, M.; Schoenborn, B.; Howell, E. E.; Dealwis, C. *Proc. Natl. Acad. Sci. U.S.A.* **2006**, *103*, 18493–18498.
(27) Bode, W.; Meyer, E., Jr.; Powers, J. C. *Biochemistry* **1989**, *28*, 1951–1963.
(28) Kossiakoff, A. A.; Spencer, S. A. *Nature* **1980**, *288*, 414–416.
(29) Kossiakoff, A. A.; Spencer, S. A. *Biochemistry* **1981**, *20*, 6462–6474.

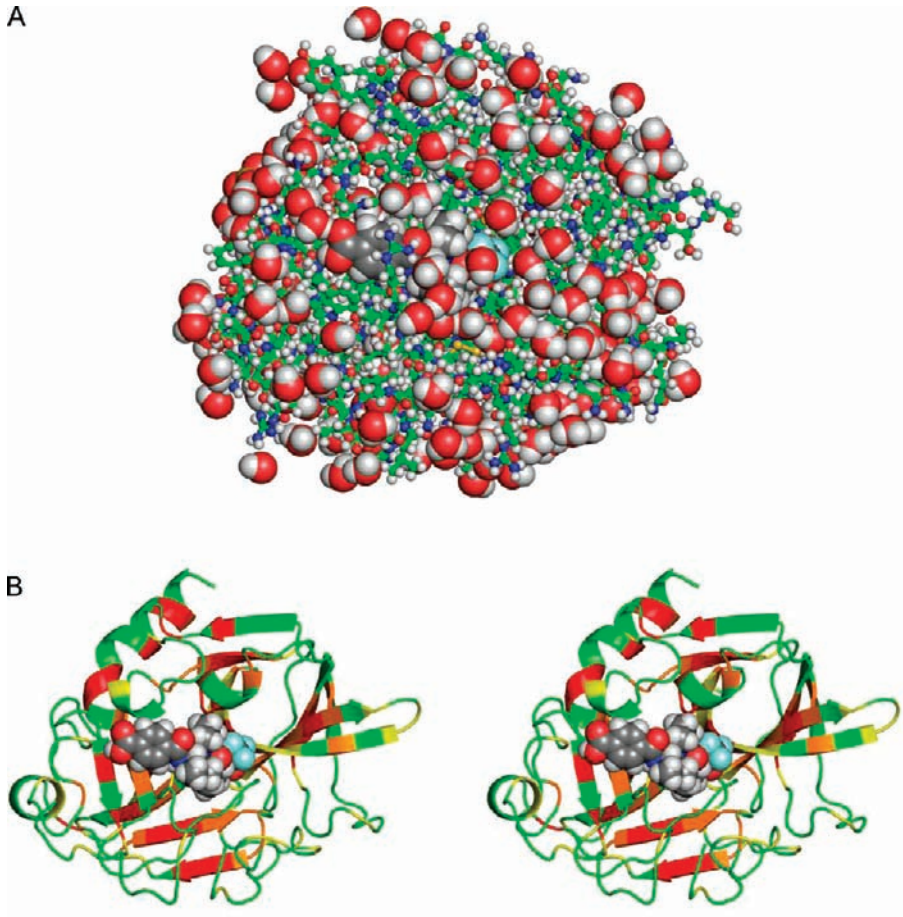

Figure 1. Overall structure of the complex between PPE and peptidic inhibitor FR130180. (A) Ball and stick model. FR130180, ions and water molecules are shown by space-filling representation. Hydrogen and deuterium atoms are colored in white. Carbon atoms of PPE and FR130180 are colored in green and gray, respectively. Oxygen, nitrogen, sulfur and fluorine atoms are colored in red, blue, yellow and light blue, respectively. (B) Stereoview of the ribbon model. PPE are colored according to the deuterium occupancy values of backbone amide. Green, highly exchanged (occupancy = 0.7−1.0); yellow, medium exchanged (occupancy = 0.3−0.7); orange, low exchanged (occupancy = 0.15−0.3); and red, non-exchanged (occupancy = 0−0.15). Figures 1, 3 and 4 were prepared by the PyMOL Molecular Graphics System (DeLano Scientific, San Carlos, CA).

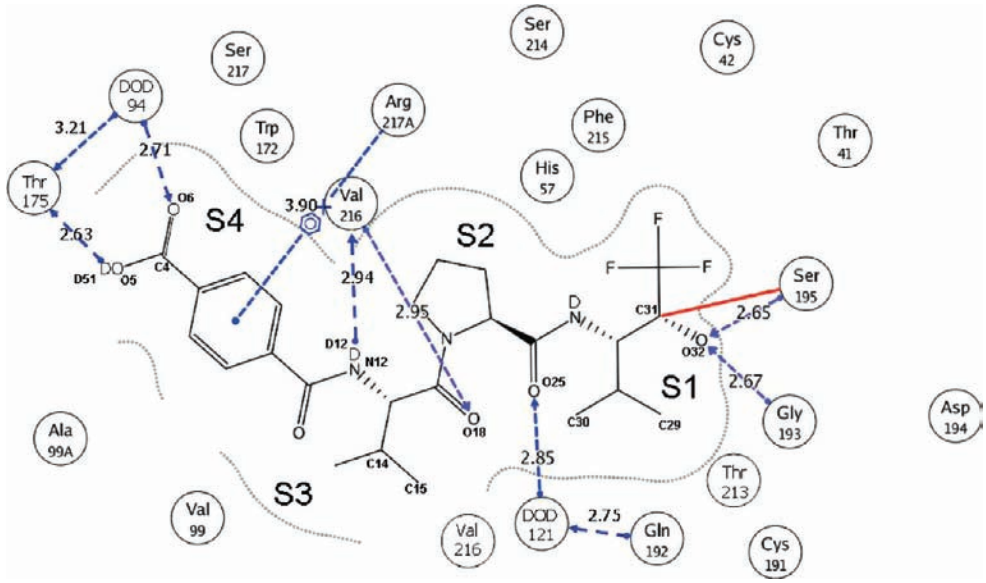

Figure 2. Schematic drawing of the interaction between PPE and FR130180. Blue dashed line with arrow, hydrogen bonds (arrow indicates the direction from donor to acceptor); blue dashed line with symbols of plus and benzene ring, cation−π interaction; and red solid line, covalent bond. The values on dash lines stand at bond distances (Å). This figure was drawn by the program MOE (Chemical Computing Group, Inc., Montréal, Québec, Canada).

and 3.64/3.90 Å apart from the Cγ1 and Cγ2 atom of Val216 in the subangstrom X-ray/neutron structure, respectively. The Cγ2 atom of Val216 is positioned at a distance of 3.86/3.98 Å from the C14 atom in the isopropyl group of the P3 position.

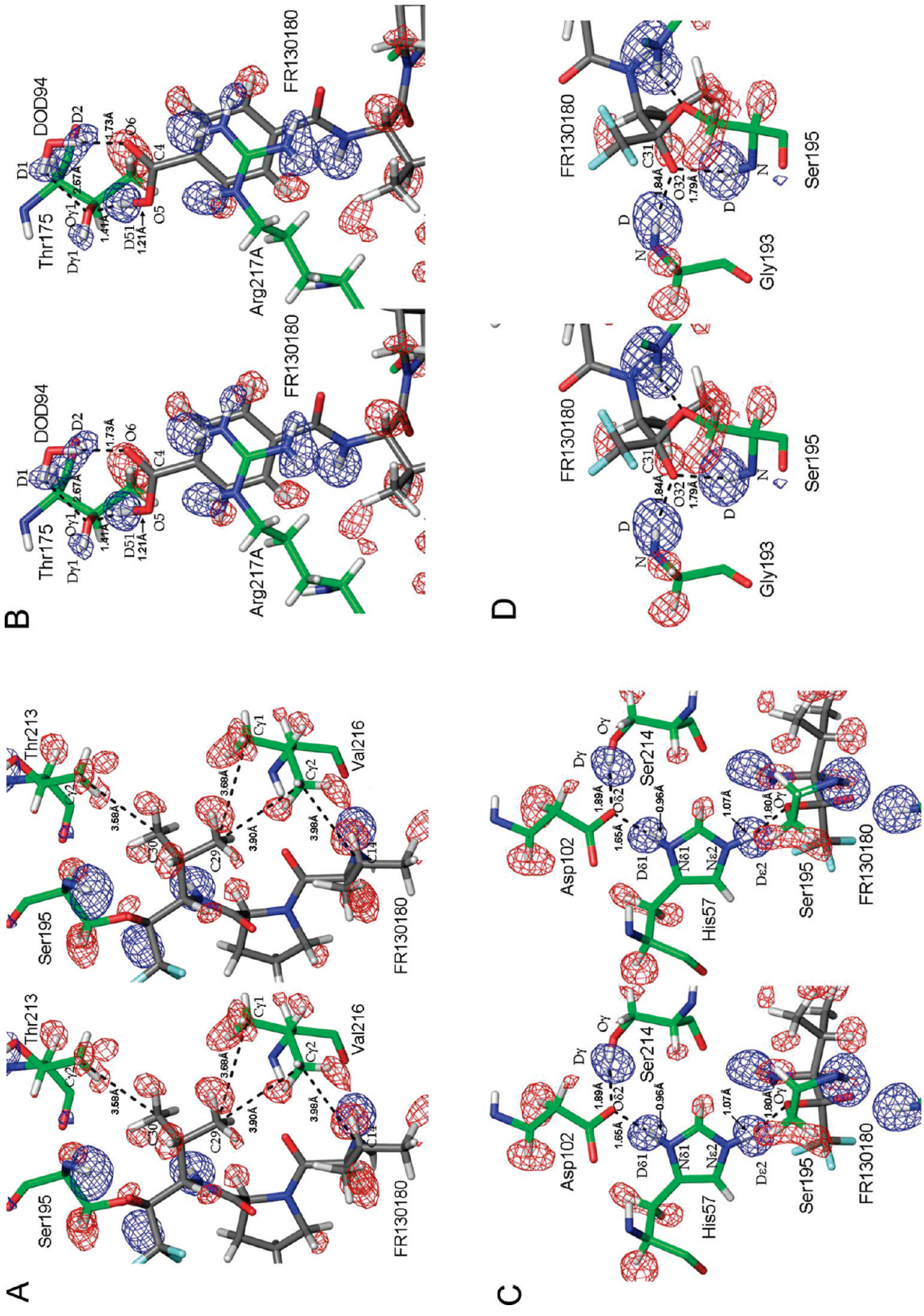

Figure 3. Nuclear density map of the PPE/FR130180 complex at 1.65 Å resolution. (A) S1 and S3 subsites. (B) S4 subsite. (C) The catalytic triad. (D) The oxyanion hole. The $F_o - F_c$ nuclear maps were calculated without hydrogens and deuteriums. The blue and red contours show +5.0 and −4.5 σ densities, respectively.

Table 2. Direct and Water Mediated Hydrogen Bonds between PPE and FR130180[a]

subsite	donor atom	D(H) atom	acceptor atom	distance[b] (Å)	distance[c] (Å)	angle[d] (deg)
S1	Gly193 N	Gly193 D(H)	FR130180 O32	2.67	1.84	158
		Gly193 H		2.64	1.90	144
S1	Ser195 N	Ser195 D(H)	FR130180 O32	2.65	1.79	157
		Ser195 H		2.64	1.86	151
S2	DOD121 O	DOD121 D2	FR130180 O25	2.85	1.92	155
	HOH159 O	–		2.60	–	–
S3	Val216 N	Val216 D(H)	FR130180 O18	2.95	2.10	161
		Val216 H		2.94	2.10	164
S3	FR130180 N12	FR130180 D(H)12	Val216 O	2.94	2.11	158
		FR130180 H12		3.04	2.21	162
S4	FR130180 O5	FR130180 D51	Thr175 Oγ1	2.63	1.41	170
		–		2.62	–	–
S4	DOD94 O	DOD94 D2	FR130180 O6	2.71	1.73	168
	HOH114 O	–		2.72	–	–

[a] Upper row, neutron (1.65 Å resolution) and lower row, X-ray (0.94 Å resolution) in a line for each subsite. [b] Distance between donor and acceptor atoms. [c] Distance between D(H) and acceptor atoms. [d] Angle of donor−D(H)−acceptor atoms.

At the S3 subsite, the amide and carbonyl groups located in the vicinity of the P3 position of FR130180 show a hydrogen bonding interaction with the backbone N and O atoms of Val216, which were confirmed in the nuclear and subangstrom electron density maps. The geometries of hydrogen bonds between PPE and FR130180 are summarized in Table 2. The interacting manner of these two hydrogen bonds is similar to that of an antiparallel β-sheet. At the S2 subsite, a water molecule mediated a hydrogen bonding interaction with the side chain of Gln192 and an aminocarbonyl moiety located between the P1 and P2 positions of FR130180.

At the S4 subsite, the guanidino group in the side chain of Arg217A located on the terminal benzoic acid moiety of FR130180 to form a cation$-\pi$ interaction (Figure 3B). The dihedral angle between the guanidino group and benzoyl ring is 164°. The distance between the Cζ atom of Arg217A and the center of the benzoyl ring is 3.90 Å. The $F_o - F_c$ nuclear density calculated without hydrogen atoms in the model structure exhibits the guanidino group of Arg217A becoming positively charged. We also found clear nuclear density belonging to a deuterium atom between Oγ1 atom of Thr175 and the terminal benzoic acid moiety of FR130180 (Figure 3B). Nuclear density shows that the carboxyl group in benzoic acid of FR130180 is in the protonated state. The bond length between the carboxyl carbon (C4) and the hydroxyl oxygen (O5) is longer than that between C4 and the carbonyl oxygen (O6). The C4−O5 and C4−O6 distances are 1.28 and 1.21 Å in the neutron structure. Subangstrom X-ray structure from nonrestrained refinement shows that both distances are 1.29 and 1.25 Å, respectively. There were two hydrogen bonds located at the benzoic acid moiety of FR130180. One is the hydrogen bond between protonated site of carboxyl group of the benzoic acid of FR130180 and the hydroxyl group of Thr175. The other is the hydrogen bond between a water molecule (DOD94) and deprotonated site of carboxyl group of the benzoic acid (Figure 3B). DOD94 is also situated in the hydrogen bond from the hydroxyl group of Thr175. The geometries of these hydrogen bonds are shown in Table 2.

Catalytic Site of PPE. The $F_o - F_c$ nuclear density maps calculated without hydrogen atoms in the model structure in the region of the catalytic triad near the S1 subsite indicated the double protonated state of imidazole ring of His57 and dissociated state of carboxyl group of Asp102 (Figure 3C). Subangstrom X-ray analysis also suggests a double protonated state for His57 (Figure 4A) and shows that the bond length between the carbon atom (Cγ) and the two oxygen atoms (Oδ1 or Oδ2) in Asp102 are nearly equivalent (Cγ−Oδ1, 1.26 Å and Cγ−Oδ2, 1.28 Å). A hydrogen bond is formed between the Nδ1 atom of His57 and the Oδ2 atom of Asp102. The detail geometries of this hydrogen bond are shown in Table 1 with that of X-ray structure at 0.94 Å resolution. The Oδ2 of Asp102 also formed hydrogen bond with a hydroxyl group of Ser214 (Figure 3C). The Dγ atom of Ser214 is 0.86 and 1.89 Å apart from the Oγ atom of Ser214 and the Oδ2 atom of Asp102, respectively. The hydrogen bond angle of Oγ−D$\gamma\cdots$Oδ2 is 162°. The Nε2 of His57 is situated in the hydrogen bond from the ester oxygen atom (Oγ) of Ser195, which is covalently bound to carbonyl carbon (C31) in an oxopropyl moiety of FR130180. The Dε2 of His57 is 1.07 and 1.80 Å apart from the Nε2 atom of His57 and the Oγ of Ser195. The hydrogen bond angle of Nε2−Dε2$\cdots$Oγ is 151°.

Since FR130180 is a covalently bound inhibitor to PPE, the carbonyl carbon (C31) of the oxopropyl moiety in FR130180 is located at the center of tetrahedral structure (Figure 3D). All angles from one vertex to the center of the tetrahedron to another vertex were around 110°. The carbonyl oxygen (O32) of the oxopropyl group is converted to a hydroxyl oxygen that interacts with the oxyanion hole comprising two hydrogen atoms from the backbone amides of Gly193 and Ser195. These two hydrogen atoms (deuterium in the neutron structure) are clearly confirmed in the $F_o - F_c$ nuclear density maps (Figure 3D), whereas the hydrogen atom from the backbone amide of Gly193 could not be observed in the $F_o - F_c$ electron density maps (Figure 4B). The hydrogen or deuterium atom bound to the O32 atom is not confirmed in nuclear maps (Figure 3D). The location of the O32 atom in the neutron structure is 1.84 and 1.79 Å from the deuterium atom of backbone amides of Gly193 and Ser195, respectively (Table 2). The distance between the O32 atom and the C31 atom of the oxopropyl group is determined to be 1.32 Å in the subangstrom X-ray structure by nonrestrained refinement.

Discussion

The crystal structure of PPE in complex with peptidic inhibitor FR130180 including the locations of the hydrogen and deuterium atoms determined by the collaborative use of both 1.65 Å resolution neutron diffraction and 1.20 Å resolution X-ray diffraction data helps us to understand catalytic mechanism and inhibitor recognition of PPE in detail. This neutron structure is also compared with those determined by subangstrom (0.94 Å) X-ray structure.

The FR130180 complex structure mimics the tetrahedral transition intermediate in the catalytic reaction. The nuclear density maps show the double protonated state of imidazole ring of His57 and dissociated state of the carboxyl group of

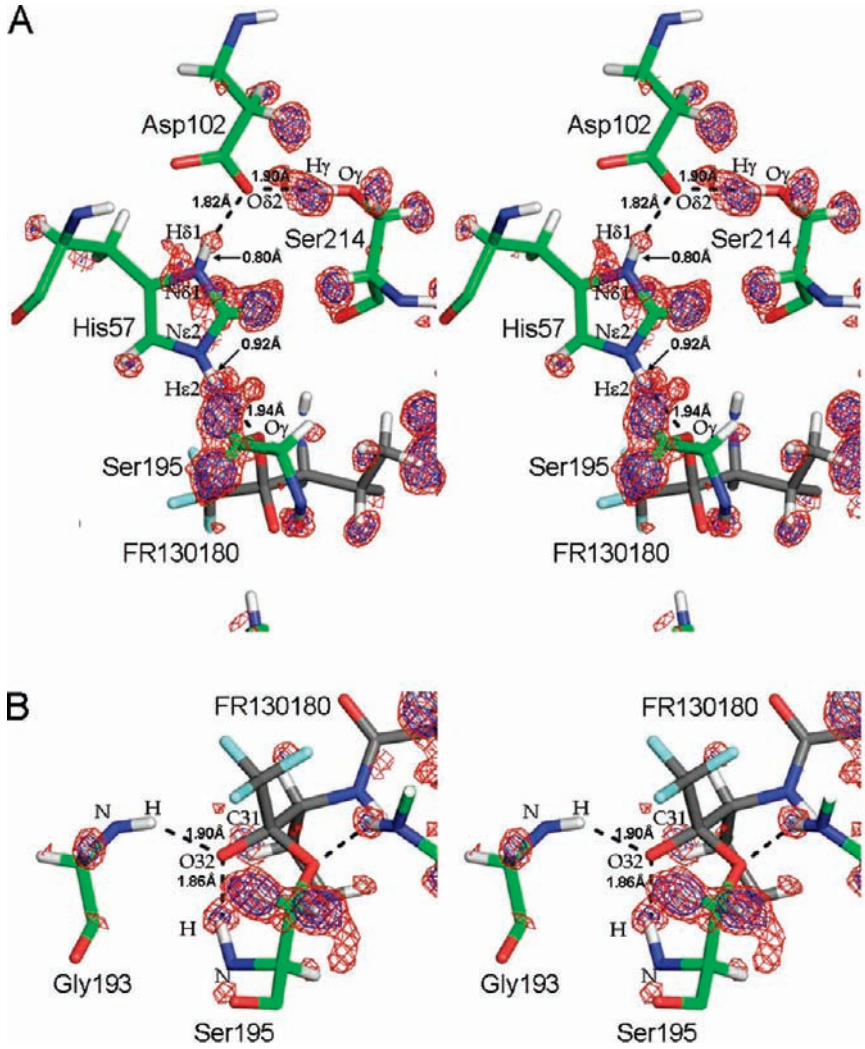

Figure 4. Electron density map of the PPE/FR130180 complex at 0.94 Å resolution. (A) The catalytic triad. (B) The oxyanion hole. The $F_o - F_c$ electron maps were calculated without hydrogens. The blue and red contours show +2.5 and +2.0 σ densities, respectively.

Asp102 clearly as seen in the neutron structure of the bovine trypsin in complex with nonpeptidic inhibitor.[28,29] The distances of Nδ1−Dδ1 and Dδ1···Oδ2 between His57 and Asp102 in the PPE/FR130180 structure are similar to those in the previously reported bovine trypsin/inhibitor complex, although the angle of Nδ1−Dδ1···Oδ2 (172°) in the PPE structure is close to linear geometry in contrast to the angle observed in trypsin structure (137°) (Table 1). The geometries of the hydrogen bond between His57 and Asp102 are summarized in Table 1 with those in other subangstrom X-ray structures of serine proteases archived in Protein Data Bank (PDB). The 2.60 Å distance between Nδ1 of His57 and Oδ2 of Asp102 in PPE/FR130180 complex in both neutron and subangstrom X-ray structures suggested to be a LBHB according to the previous definition. Formation of a LBHB requires a donor−acceptor distance of less than 2.65 Å for a nitrogen−oxygen pair by X-ray diffraction studies and ΔpK_a between the proton donor and acceptor at or near zero.[4,5,30] The distance between Nδ1 and Dδ1 atoms is, however, 0.96 Å in the neutron structure and 0.80 Å in the X-ray structure. The slightly longer distance in neutron structure is characteristic in comparison with X-ray structure.[31] These distances in PPE/FR130180 complex are similar to those in αLP without inhibitor, but are somewhat shorter than those in subtilisin (Table 1). Fuhrmann and co-workers concluded the His57[Nδ1]···Asp102[Oδ2] hydrogen bond is a normal ionic hydrogen bond in their structures.[10] They also proposed a short ionic hydrogen bond (SIHB) between Nε2 atom of His57 and carbonyl oxygen atom (O2) in boroVal(gol) (MeOSuc-Ala-Ala-Pro-boroVal−OH), which is the transition state mimic inhibitor of αLP, stabilizing transition state. They defined that a SIHB is a hydrogen bond fulfilling the donor−acceptor distance requirement of a LBHB, but for which the hydrogen atom is localized on the donor atom. The His57[Nε2]···boroVal(gol)[O2] and His57[Nε2−Dε2] distances were 2.64 and 0.91 Å, respectively, in the literature. According to their definition, the hydrogen bond between Nδ1 of His57 and Oδ2 of Asp102 in PPE/FR130180 complex is categorized as SIHB, not LBHB. The Oδ2 of Asp102 also formed a hydrogen bond with a hydroxyl group of Ser214 (Figures 3C and 4A). The hydrogen bond between the side chain of Asp102 and Ser214 is hypothesized to generate a polar environment for catalytic Asp102 of trypsin.[32] The strength of a short hydrogen bond becomes weaker in the polar environment of Asp102.[33] On the other hand, it may be less of a polar environment around His57

(30) Hibbert, F.; Emsley, J. *Adv. Phys. Org. Chem.* **1990**, *26*, 255–379.
(31) Wilson, C. C. *Single Crystal Neutron Diffraction from Molecular Materials*; World Scientific: Singapore, 2000.
(32) McGrath, M. E.; Vásquez, J. R.; Craik, C. S.; Yang, A. S.; Honig, B.; Fletterick, R. J. *Biochemistry* **1992**, *31*, 3059–3064.
(33) Kim, Y.; Lim, S.; Kim, Y. *J. Phys. Chem. A* **1999**, *103*, 6632–6637.

in PPE/FR130180 complex because the Oγ atom of Ser195 is an ether oxygen, which is less polar than a hydroxyl oxygen. This polar deviation in catalytic triad of PPE/FR130180 complex may affect the formation of a SIHB between the side chains of His57 and Asp102.

Neutron structure analysis indicates the carboxyl oxygen (O32) of the oxopropyl group of FR130180 is present as an oxygen anion (oxyanion). In contrast, the subangstrom X-ray structure of the αLP/boroVal(gol) complex shows that there is no oxyanion, but a hydroxyl group in a transition-state analogue.[10] In the PPE/FR130180 complex structure, the deuterium atom bound to the O32 atom of the oxopropyl group of FR130180 is not observed in the $F_o - F_c$ nuclear map calculated without hydrogens (Figure 3D), indicating that O32 atom is an oxyanion. This is the first case that an oxyanion of a tetrahedral intermediate analogue is directly observed at an oxyanion hole. The carbonyl oxygen of the substrate is known to be activated to form a tetrahedral intermediate during catalysis by binding to the oxyanion hole which stabilizes the oxyanion.[34] The existence of an oxyanion created from a hydroxyl group suggests that the oxyanion is stabilized by the structural characteristics of the oxyanion hole. In the PPE/FR130180 complex structure, C31 and O32 atoms in FR130180 and the nitrogen and deuterium (hydrogen) atoms of backbone amides of Gly193 and Ser195 are almost in one plane (Figures 3D and 4B). The angles of C31−O32···[Gly193]D(H), C31−O32···[Ser195]D(H), and [Gly193]D(H)···O32···[Ser195]D(H) are 134°, 119°, and 105° in the neutron structure, respectively. In general, the oxyanion is tetrahedral with three lone pairs occupying an sp^3 orbital. However, the angles around O32 atom show that O32 atom locates in the center of a trigonal, not tetrahedral conformation. The carbonyl oxygen is trigonal planar with two lone pairs occupying an sp^2 orbital. The distance between C31 and O32 is 1.32 Å in the subangstrom X-ray structure by nonrestrained refinement. This distance corresponds to the medium value between typical distances of C═O (1.21 Å) and C−OH (1.43 Å) bonds.[35] The conformation around the oxyanion hole in the PPE/FR130180 complex shows that the oxyanion O32 atom may be intermediate between sp^2 and sp^3 orbital geometry. This conformation is suitable for stabilization of the oxyanion because two lone pairs of the oxyanion are directed toward the deuterium (hydrogen) atoms of backbone amides of Gly193 and Ser195.

PPE recognized PR130180 at two isopropyl groups through hydrophobic interactions which are suggestive of a leucine zipper-like structure (Figure 3A). The C29 and C30 atoms in isopropyl group at the P1 position is almost located at the "R_{min}" distance (3.53 Å between two carbons), which is the distance at the minimum of the 6-12 type van der Waals potential proposed by Levitt,[36] from the Cγ2 atom of Val216 (C−C distance: 3.64/3.68 Å in X-ray/neutron structure) and the Cγ2 atom of Thr213 (C−C distance: 3.53/3.58 Å), respectively. The isopropyl group at the P1 position mimics the valine residue which is the specific residue of recognition by elastase. The strong van der Waals interaction confirmed at S1 subsite in PPE/FR130180 complex may influence the substrate specificity of elastase. Furthermore, the sequential hydrophobic interaction consisting of Thr213, P1, Val216, and P3 might allow the substrate binding in the recognition sites of the enzyme to be stabilized by long-range dispersion force.

At the S4 subsite, we confirmed two interesting features of inhibitor recognition by PPE. One is the cation−π interaction formed between the guanidino group of Arg217A and the benzoyl ring in FR130180 (Figure 3B). The cation−π interaction is known as a stronger interaction than the $\pi-\pi$ interaction.[37] In protein structures, cation−π interactions are found to be common and strong interactions when a cationic side chain (Lys or Arg) is near an aromatic side chain (Phe, Tyr, or Trp).[38] The average B-factors of the guanidino group of Arg217A and the benzoyl ring in FR130180 are 16.0 $Å^2$ and 9.7 $Å^2$ in neutron, and 8.2 $Å^2$ and 5.6 $Å^2$ in subangstrom X-ray structures, respectively. These values are comparable to those of the whole protein (14.0 $Å^2$ in neutron and 8.6 $Å^2$ in X-ray) and FR130180 (9.6 $Å^2$ in neutron and 5.7 $Å^2$ in X-ray), respectively. Another interesting interaction involves the hydrogen bond between the hydroxyl group of Thr175 and the carboxyl group in benzoic acid of FR130180. The carboxyl group in benzoic acid of FR130180 is the protonated state (Figure 3B). The deuterium atom (D51) in the protonated site of carboxyl group is 1.21 and 1.41 Å apart from the O5 atom of FR130180 and the Oγ1 atom of Thr175, respectively. This O−D distance in the protonated carboxyl group is slightly longer than the typical O−H distance (1.02 Å) in protonated carboxyl group.[35] The donor−acceptor (O5···Oγ1) distance (2.63 Å) between FR-130180 and Thr175 well agrees with the characteristic O···O distance of resonance-assisted hydrogen bond (RAHB), which is one of the strong hydrogen bonds.[39] A water molecule, DOD94 in neutron structure, is also concerned with the interaction between Thr175 and benzoic acid of FR130180. It is thought that these strong interactions between PPE and the benzoic acid moiety of FR130180 were important for inhibitor recognition by PPE.

Conclusion

Neutron diffraction data has, for the first time, visualized a SIHB formed between catalytic residues His57 and Asp102, as well as the oxyanion located at the oxyanion hole, and has identified strong hydrogen bonds as contributing to inhibitor recognition in PPE. These are fundamentally important structural data for the catalytic reaction and molecular recognition of an enzyme, as shown in the case of HIV-1 protease.[40]

Acknowledgment. We thank Drs. N. Shimizu, M. Kawamoto, and M. Yamamoto of SPring-8 (proposal No. 2005B0982) and Profs. N. Igarashi and S. Wakatsuki of Photon Factory (proposal No. 2008G075) for X-ray data collection. We are also indebted to Prof. B. W. Matthews for critical reading of this manuscript. This work was supported in part by MEXT, Grant-in-Aid for Scientific Research (B) (19370046) (to R.K.).

Supporting Information Available: A table of conditions of data collection and statistics of data processing and refinement in the X-ray/neutron diffraction analysis for PPE. This material is available free of charge via the Internet at http://pubs.acs.org.

JA9028846

(34) Robertus, J. D.; Kraut, J.; Alden, R. A.; Birktoft, J. J. *Biochemistry* **1972**, *11*, 4293–4303.
(35) Watson, D. G.; Brammer, L.; Orpn, A. G.; Taylor, R. *International Tables for Crystallography Vol. C*; Kluwer Academic Publishers: Dordrecht, The Netherlands, 1992.
(36) Levitt, M. *J. Mol. Biol.* **1974**, *82*, 393–420.
(37) Anslyn, E. V.; Dougherty, D. A. *Modern Physical Organic Chemistry*; University Science Books: Sausalito, CA, 2004.
(38) Gallivan, J. P.; Dougherty, D. A. *Proc. Natl. Acad. Sci. U.S.A.* **1999**, *96*, 9459–9464.
(39) Gilli, P.; Bertolasi, V.; Ferretti, V.; Gilli, G. *J. Am. Chem. Soc.* **1994**, *116*, 909–915.
(40) Adachi, M.; Ohhara, T.; Kurihara, K.; Tamada, T.; Honjo, E.; Okazaki, N.; Arai, S.; Shoyama, Y.; Kimura, K.; Matsumura, H.; Sugiyama, S.; Adachi, H.; Takano, K.; Mori, Y.; Hidaka, K.; Kimura, T.; Hayashi, Y.; Kiso, Y.; Kuroki, R. *Proc. Natl. Acad. Sci. U.S.A.* **2009**, *106*, 4641–4646.